



## *Propionibacterium acnes* inhibits FOXM1 and induces cell cycle alterations in human primary prostate cells<sup>☆</sup>

Behnam Sayanjali<sup>a</sup>, Gitte J.M. Christensen<sup>b</sup>, Munir A. Al-Zeer<sup>a</sup>,  
Hans-Joachim Mollenkopf<sup>a</sup>, Thomas F. Meyer<sup>a,\*</sup>, Holger Brüggemann<sup>b</sup>

<sup>a</sup> Department of Molecular Biology, Max Planck Institute of Infection Biology, Berlin, Germany

<sup>b</sup> Department of Biomedicine, Aarhus University, Aarhus, Denmark



### ARTICLE INFO

#### Article history:

Received 13 May 2016

Received in revised form 17 June 2016

Accepted 27 June 2016

#### Keywords:

Primary prostate epithelial cells

*Propionibacterium acnes*

Cell cycle

FOXM1

Berninamycin

Thiopeptide

### ABSTRACT

*Propionibacterium acnes* has been detected in diseased human prostate tissue, and cell culture experiments suggest that the bacterium can establish a low-grade inflammation. Here, we investigated its impact on human primary prostate epithelial cells. Microarray analysis confirmed the inflammation-inducing capability of *P. acnes* but also showed deregulation of genes involved in the cell cycle. qPCR experiments showed that viable *P. acnes* downregulates a master regulator of cell cycle progression, FOXM1. Flow cytometry experiments revealed that *P. acnes* increases the number of cells in S-phase. We tested the hypothesis that a *P. acnes*-produced berninamycin-like thiopeptide is responsible for this effect, since it is related to the FOXM1 inhibitor siomycin. The thiopeptide biosynthesis gene cluster was strongly expressed; it is present in subtype IB of *P. acnes*, but absent from type IA, which is most abundant on human skin. A knock-out mutant lacking the gene encoding the berninamycin-like peptide precursor was unable to downregulate FOXM1 and to halt the cell cycle. Our study reveals a novel host cell-interacting activity of *P. acnes*.

© 2016 The Authors. Published by Elsevier GmbH. This is an open access article under the CC BY-NC-ND license (<http://creativecommons.org/licenses/by-nc-nd/4.0/>).

### 1. Introduction

Propionibacteria can be found as part of the skin microbiota on almost every human being. In particular, *P. acnes* successfully and often exclusively colonizes sebaceous follicles of the face and back. In the last decade, improved microbial cultivation approaches, genome sequencing, phylotyping efforts, host-bacterium interaction studies, and animal experiments have revealed that *P. acnes* can act as an opportunistic pathogen (Brüggemann et al., 2004; Brzuszkiewicz et al., 2011; Fitz-Gibbon et al., 2013; Kistowska

et al., 2014; Lomholt and Kilian, 2010; McDowell et al., 2012, 2013; Olsson et al., 2012; Perry and Lambert, 2011; Shinohara et al., 2013). At the same time, new findings regarding the possible beneficial role of *P. acnes* for the host have been made, and the microbial interactions with the host immune system have been highlighted (Agak et al., 2014; Belkaid and Segre, 2014; Kistowska et al., 2014, 2015; Qin et al., 2014). Apart from its association with the highly prevalent skin disorder acne vulgaris, there is accumulating evidence for a role of *P. acnes* in the pathogenesis at non-skin sites, e.g. with respect to postoperative and device-related infections, including those of joint prostheses, shunts and prosthetic heart valves. Circumstantial evidence exists for a role in cases of endocarditis, post-neurosurgical central nervous system infections, dental infections, bacterial endophthalmitis, postoperative spine infections and sarcoidosis (Eishi, 2013; Perry and Lambert, 2011).

Another association concerns prostate pathologies: several studies reported the isolation and cultivation of *P. acnes* from radical prostatectomy specimens, and its visualization in cancerous tissue (Alexeyev et al., 2007; Bae et al., 2014; Cohen et al., 2005; Fassi Fehri et al., 2011). *In vitro* experiments showed that *P. acnes* triggered the secretion of cytokines and chemokines such as interleukin (IL)-6, IL-8 and GM-CSF in RWPE-1 cells, a prostate epithelial cell line that was immortalized with human papillomavirus 18

<sup>☆</sup> Microarray data from this publication has been deposited in NCBI's Gene Expression Omnibus (GEO, <http://www.ncbi.nlm.nih.gov/geo/>) and are accessible through GEO Series accession number GSE72585. Reviewer access link: <http://www.ncbi.nlm.nih.gov/geo/query/acc.cgi?token=ihaloakcjdmrjal&acc=GSE72585>.

\* Corresponding author at: Max Planck Institute for Infection Biology, Charitéplatz 1, 10117 Berlin, Germany.  
E-mail address: [meyer@mpiib-berlin.mpg.de](mailto:meyer@mpiib-berlin.mpg.de) (T.F. Meyer).

(Bae et al., 2014; Drott et al., 2010; Fassi Fehri et al., 2011). In these cells, *P. acnes* induced a delayed but sustained inflammation, which was associated with prolonged NF-κB activation (Mak et al., 2012). Moreover, infection with *P. acnes* modulates adhesion and proliferation properties of RWPE-1 cells, which results in the initiation of cellular transformation (Fassi Fehri et al., 2011). Immunofluorescence and electron microscopy has demonstrated bacterial invasion and intracellular persistence of *P. acnes* (Fassi Fehri et al., 2011; Mak et al., 2012). In animal experiments the bacterium was able to induce a persistent infection of the prostate gland (Olsson et al., 2012; Shinohara et al., 2013). Despite this circumstantial evidence, the role of *P. acnes* in prostate pathologies is a matter of controversy. It is possible that the pathogen might colonize the anaerobic zones of an existing prostate tumor and/or might be introduced during surgery or during previous surgical intervention, since patients who undergo radical prostatectomy usually undergo multiple biopsy procedures beforehand.

Here, we wanted to investigate the host response to exposure of *P. acnes* in a primary prostate cell model that mimics a possible *in vivo* encounter with *P. acnes* more accurately than an immortalized cell culture model. We found that *P. acnes* can act as a pro-inflammatory stimulus as well as a cell cycle disrupter. Evidence for a possible mechanism for cell cycle interference involving a *P. acnes*-produced thiopeptide is presented and the *in vivo* relevance of our findings is discussed.

## 2. Material and methods

### 2.1. Antibodies

Polyclonal anti-*P. acnes* antibody 1:100 (Fassi Fehri et al., 2011), Anti-EPCAM (Epithelial cell adhesion molecule) (1:200, BD Biosciences), Anti-E-cadherin (1:200, BD Biosciences), and anti-rabbit IgG secondary antibody (1:150, Jackson ImmunoResearch) were used for immunofluorescence analysis. For immunoblotting, polyclonal rabbit antibodies against Aurora B/AIM1, PLK1 and CCNB1 (1:1000, Cell Signaling), FOXM1 (K-19 Santa Cruz, 1:1000), mouse monoclonal anti-p53 (DO-1, Santa Cruz, 1:500) and monoclonal anti-B-actin antibody (1:5000, Sigma-Aldrich) were used. Anti-mouse and anti-rabbit secondary antibodies (Amersham) were diluted 1:2000 for western blotting.

### 2.2. Cell culture and bacteria

Human primary prostate epithelial cells (PrEC, Lonza, CC-2555) were cultured in PrEGM complete medium (CC-3166) supplemented with bovine pituitary extract (BPE), epidermal growth factor, insulin, hydrocortisone, retinoic acid, transferrin, triiodothyronine and epinephrine, at 37 °C in a humidified incubator containing 5% CO<sub>2</sub>. Three *P. acnes* wild type strains were used, KPA171202 (type IB; DSMZ, no. 16379) (Brüggemann et al., 2004) *P. acnes* strain P6 (type IB, strain collection no. X524), an isolate from a cancerous prostate (Fassi Fehri et al., 2011; Mak et al., 2013) and *P. acnes* strain 266 (type IA) (Brzuszkiewicz et al., 2011). All strains were cultured on Brucella agar plates for 4 days at 37 °C under anaerobic conditions. For heat inactivation, *P. acnes* was incubated at 60 °C for 30 min.

### 2.3. Mutagenesis of *P. acnes*

The thiopeptide knockout mutant (strain collection no. X551) was generated as described previously (Sørensen et al., 2010). Strain *P. acnes* KPA171202 was used as the wild-type strain and *Escherichia coli* DH5α was used as a recipient in all cloning steps. In brief, a 583 bp upstream and a 547 bp downstream region of the thiopeptide precursor encoding gene (*berA1*) were amplified

using the primer combinations Thio\_1/Thio\_2 and Thio\_3/Thio\_4, respectively (Supplementary Table 2). The fragments were gel-purified, digested with Acc65I and ligated. After column purification of the ligation mixture (QIAquick, Qiagen) a PCR was carried out using the ligation mixture as a template with the primer combination Thio\_1/Thio\_4. The approx. 1 kb product was gel-purified and cloned into pGEM-T-easy. Positive *E. coli* DH5α clones were obtained and isolated plasmids were tested for the correct insert by restriction digestion. Plasmid DNA was subsequently digested with Acc65I and ligated with the Acc65I-digested fragment containing the erythromycin-resistance cassette; This fragment was amplified using genomic DNA of *Saccharopolyspora erythraea* (DSM no. 40517) as a template using the primers ermE.for and ermE.rev. The ligation mixture was transformed into *E. coli* DH5α. Ampicillin (100 µg/ml)-resistant clones were obtained. Prior to electroporation into *P. acnes* KPA171202, plasmid DNA was extracted from positive clones and transformed into the dam-negative *E. coli* strain GM2199. Competent cells of *P. acnes* KPA171202 were prepared as described previously (Sørensen et al., 2010). Electrocompetent *P. acnes* cells were freshly prepared before the electroporation, which was carried out using a Gene Pulser (BioRad) and 0.1 cm electroporation cuvettes. Plasmid DNA (6 µg; isolated from the dam-negative *E. coli* strain GM2199) was added to 50 µl competent *P. acnes* cells. Gene Pulser settings of 50 µF, 400 Ω, and 1.5 kV were used. Subsequently, cells were recovered in 1 ml pre-warmed BHI medium, and centrifuged (5 min, 3000g). The resulting pellet was resuspended in 100 µl BHI medium and plated out on a Brucella agar plate without any antibiotics. The plate was incubated for 24 h at 37 °C under anaerobic conditions. The following day, bacteria were harvested using a sterile cotton swab, resuspended and washed in pre-warmed BHI medium and re-plated on Brucella plates containing 10 µg/ml erythromycin, and incubated for 4–6 days. All clones obtained were tested by PCR to validate the correct knock-out of the thiopeptide precursor encoding gene.

### 2.4. RNA preparation and RNA-seq

Total RNA from *P. acnes* (strain KPA171202) grown under anaerobic conditions to the exponential and stationary growth phase in BHI medium at 37 °C was prepared with the RNA PowerSoil®/Total RNA Isolation Kit (Mo-Bio, USA), following manufacturer instructions. RNA quality was controlled using the Bioanalyzer (Agilent Technologies, USA).

The cDNA libraries were constructed by Vertis Biotechnology AG, Germany, as previously described (Dugar et al., 2013; Sharma et al., 2010). The cDNA libraries were sequenced using a HiSeq 2000 machine (Illumina) in single-read mode and 100 cycles. Detailed descriptions of procedures used for quality control, read mapping, expression graph construction and normalization of expression graphs have been published previously (Dugar et al., 2013). For graph visualization the Integrative Genome Browser (IGB version 8.5.4) was used (Nicol et al., 2009).

### 2.5. Infection of prostate epithelial cells

*P. acnes* wild-type and mutant strains were harvested from Brucella plates, washed in the respective cell culture medium and diluted. Viability of bacteria was assessed by colony-forming unit (CFU) counts; CFU counts ascertained that *P. acnes* was viable in the cell culture medium used over the indicated infection time periods. PrEC cells were seeded into six-well plates. Cells were infected 48 h later with *P. acnes* strains at MOI 100 for short-term infections (24 h and 48 h) and MOI 30 for long-term infection (2 weeks) in a humidified 5% CO<sub>2</sub> atmosphere at 37 °C. For long-term infection the medium was replaced every 48 h and the cells were passaged after one week.

## 2.6. Host cell viability

A WST-1 assay (WST-1 Cell Proliferation Kit, Abcam) was used to determine host cell viability in the absence and presence of *P. acnes*. The assay measures the activity of cellular mitochondrial dehydrogenases that can cleave the tetrazolium salt WST-1 to formazan. Formazan formation was quantified by measuring the change in absorbance at 440 nm in a microplate reader (procedure as described by the manufacturer).

## 2.7. Antibiotic protection assay

Bacterial entry into host cells was quantified by antibiotic protection assay. Cells were seeded in 24-well plates prior to infection. At 24 h p.i., tetracycline (Sigma-Aldrich) was added for 2 h at a final concentration of 50 µM/ml to kill the extracellular bacteria. Cells were washed and 1% saponin (Sigma) was added to permeabilize cells, followed by plating of appropriate dilutions of lysate on Brucella agar. Assays were performed in duplicate wells. Each experiment was repeated at least three times.

## 2.8. Protein extraction, SDS-PAGE and western blotting

Cells grown in six-well plates were washed with PBS and lysed in Laemmli buffer containing protease inhibitor cocktail (cComplete, Roche). Samples were boiled at 95 °C for 10 min and stored at –20 °C until required. Proteins were separated on 12% SDS-PAGE and then transferred to polyvinylidene difluoride (PVDF) membranes (PerkinElmer Life Sciences). The PVDF-membranes were blocked in 3% non-fat dry milk tris-buffered saline (containing 0.5% Tween 20) for 30 min. Membranes were probed with primary antibodies and HRP-conjugated secondary antibodies, and detected with ECL reagent (Amersham). ECL Western blotting substrate was detected by Hyperfilm ECL (Amersham Biosciences). The monoclonal anti-B-actin antibody (Sigma) was used as a loading control. All blots shown are representative of at least three independent experiments.

## 2.9. Microarray and transcriptome analysis

Microarray experiments were performed as dual-color hybridizations. To compensate for dye-specific effects, a dye-reversal color swap was applied (Churchill, 2002). Samples were isolated with TRIzol (Invitrogen) and total RNA was prepared according to manufacturer's instructions using glycogen as a carrier. The amount and purity of total RNA was assessed using an Agilent 2100 bioanalyzer (Agilent Technologies) and a NanoDrop 1000 spectrophotometer (Kisker). RNA labeling was performed with the Quick Amp Labeling Kit (Agilent Technologies). In brief, mRNA was reverse-transcribed and amplified using an oligo-dT-T7-promotor primer, and resulting cDNA was labeled with either Cyanine 3-CTP or Cyanine 5-CTP. After precipitation, purification, and quantification, 1.25 µg of each labeled cDNA was fragmented and subsequently hybridized to whole-human genome 44k microarrays (AMADID-014850 and Agilent-026652), according to the manufacturer's protocol (Agilent Technologies). Hybridized microarrays were washed using the SSC washing protocol (Agilent Technologies). Scanning of microarrays was performed with 5 µm resolution and using extended dynamic range (XDR) using a DNA microarray laser scanner (Agilent Technologies). Raw microarray image data were analyzed with the Image Analysis/Feature Extraction software G2567AA (Version A.11.5.1.1, Agilent). The extracted MAGE-ML files were further analyzed with the Rosetta Resolver BioSoftware, Build 7.2. Ratio profiles comprising single hybridizations were combined in an error-weighted fashion to create ratio experiments. A 2-fold change expression cut-off for

ratio experiments was applied together with anti-correlation of ratio profiles rendering the microarray analysis highly significant (*p*-value < 0.01), robust and reproducible. The data presented in this publication have been deposited in NCBI's Gene Expression Omnibus (GEO, <http://www.ncbi.nlm.nih.gov/geo/>) and are accessible through GEO Series accession number GSE72585. Ingenuity Pathway Analysis (IPA; <http://www.ingenuity.com>) software was used for functional analyses of transcriptome data. The tool identified the biological functions and/or diseases that were most significant to the expression data. Genes which were de-regulated at least two fold with *p*-values < 0.01 were included in the analysis and associated with biological functions and/or diseases in the Ingenuity Knowledge Base. Right-tailed Fisher's exact test was used to calculate a *p*-value determining the probability that each biological function and/or disease assigned to data sets was due to chance alone. DAVID (The Database for Annotation, Visualization and Integrated Discovery) was also used as a functional annotation tool which helps identify the biological meaning in large datasets (<https://david.ncifcrf.gov/>). For the identification of protein–protein interactions String was used (<http://string-db.org/>). Only genes which were deregulated at least 2-fold with *p*-values < 0.01 were analyzed.

## 2.10. Quantitative PCR

We evaluated the expression pattern of FOXM1 and its cell cycle-related targets before and after infection by RT-PCR. Total RNA was extracted from infected and uninfected cells using TRIzol according to manufacturer's protocol. After DNase-treatment (Invitrogen) and Bioanalyzer quality control (Agilent Technologies), the resulting RNA was used for RT-PCR validation. Reactions were prepared according to the manufacturer's protocol using SYBR Green PCR Master Mix (Applied Biosystems) and cycled on a 7900HT Real-Time PCR System (Applied Biosystems). GAPDH was used as an internal control and all reactions were run in triplicate. mRNA levels were quantified by calculating average  $2^{-\Delta\Delta Ct}$  values, where Ct is the cycle number for the control and target transcript at the chosen threshold.  $\Delta Ct = Ct_{target} - Ct_{GAPDH}$  was calculated by subtracting the average Ct of GAPDH from the average Ct of the target transcript. The relative difference in expression between infected and uninfected cells was calculated as fold change. All the primers used for this study were designed using the NCBI BLAST tool and are listed in Supplementary Table 2. These primers were designed to specifically detect all the possible isoforms of the target genes.

## 2.11. Immunofluorescence microscopy

PrEC cells were grown on autoclaved 12-mm cover slips. After *P. acnes* infection, cells were washed with PBS and fixed with 4% paraformaldehyde in PBS for 15 min at room temperature followed by three washes in PBS/0.1% Tween-20. Cells were stained by permeabilizing with 0.2% Triton X-100 for 15 min and blocking with 3% bovine serum albumin (BSA, Biomol) in PBS for 30 min, all at room temperature. Primary antibody against *P. acnes* was used at 1:100 dilution for 1 h, followed by a detection step using Cy2 or Cy3-conjugated anti-rabbit IgG secondary antibodies (1:150, 1 h). Nuclei were stained with Draq5 (Cell Signaling). Cover slips were mounted in Mowiol and analyzed by confocal laser scanning microscopy using a Leica TCS SP equipped with an argon–krypton mixed gas laser. Images were taken using appropriate excitation and emission filters for the fluorescence dyes used. Overlay images of the single channels were obtained using Adobe Photoshop.

Extra-/intracellular staining was achieved as follows: after fixation of infected cells with 4% paraformaldehyde and blocking with 3% BSA for 30 min, extracellular bacteria were stained with primary anti-*P. acnes* antibody for 1 h and subsequently detected

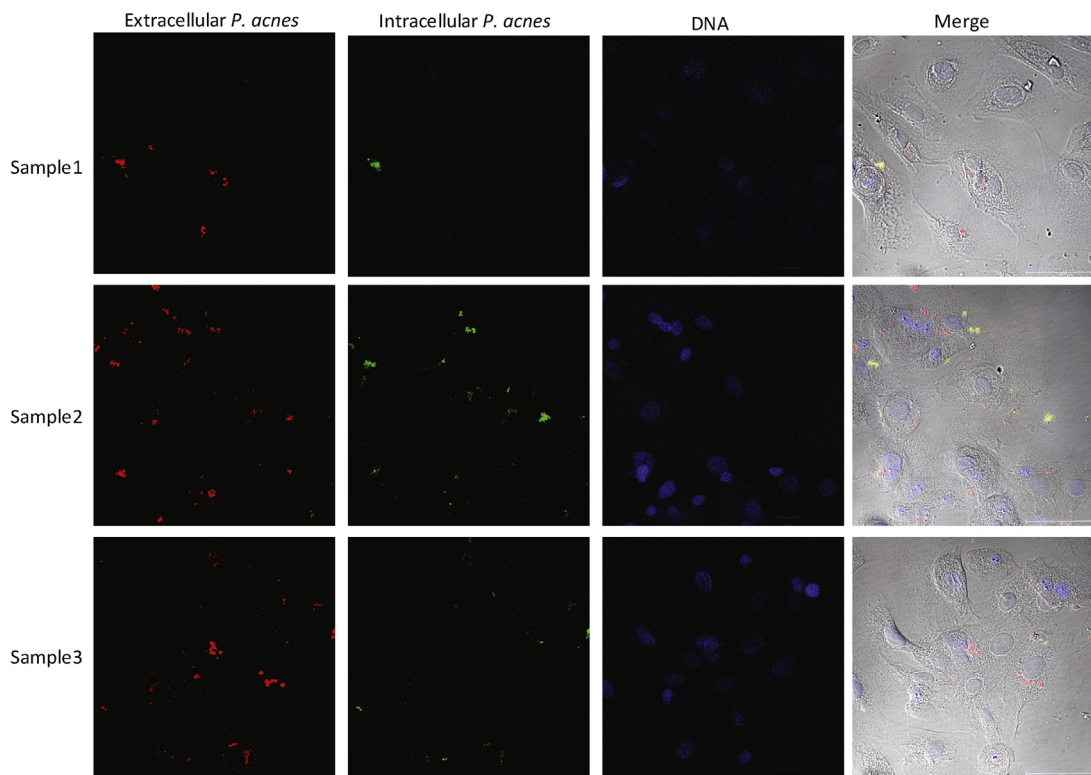


**Fig. 1.** Invasion of *P. acnes* into PrEC cells. Immunofluorescence experiments were carried out with double-staining of *P. acnes* to distinguish intra- from extracellular bacteria. Infections were performed with an MOI of 100 for 24 h. Green: extracellular *P. acnes*, red: intracellular *P. acnes*, Blue: cellular nuclei. Scale bar 50  $\mu$ m. Representative images of three independent experiments are shown.

with secondary Cy2-conjugated anti mouse IgG antibody (1:150, 1 h; Jackson ImmunoResearch). Cells were then permeabilized with 0.2% Triton X-100 for 15 min and intracellular bacteria were stained with primary anti-*P. acnes* antibody for 1 h, and detected with secondary Cy3-conjugated anti-mouse IgG antibody (1:150, 1 h; Jackson Immunoresearch). Coverslips were mounted in Mowiol and analyzed.

#### 2.12. Flow cytometry analysis

Cell cycle analysis using flow cytometry was performed by DNA content as published (Pozarowski and Darzynkiewicz, 2004). Briefly, PrEC cells were cultured in PrEGM medium and synchronized using serum starvation. Before infection with *P. acnes* the medium was replaced with medium containing serum and the infection was performed as described above. Once semi confluent, cells were detached using trypsin and fixed with 100% EtOH. Fixed cells were washed with cold PBS and DNA was stained with propidium iodide (PI, Life Technologies). Cells were then re-suspended in RSA-PI(50) buffer (PBS supplemented with 100  $\mu$ g/ml RNaseA, 2% fetal bovine serum, 0.02% NaN<sub>3</sub> and 50  $\mu$ g/ml PI), and analyzed by fluorescent flow cytometer LSRII cell analyzer. PI signal can be detected at 617 nm, at FL2 channel for FACSCalibur. The percentage of cells in each gate was then normalized against the total number of cells in each sample.

#### 2.13. Statistical analysis

The results are represented as means  $\pm$  SD. *p*-values for determining statistical significance were calculated using an unpaired two-tailed Student's *t*-test.

### 3. Results

#### 3.1. Establishment of the PrEC cell infection model

We first set up a new infection model using human primary prostate epithelial cells known as PrEC cells (Sobel et al., 2006). A primary model is better suited to mimic the *in vivo* scenario of prostate tissue exposure to *P. acnes* compared to the immortalized cancer-like cell lines used previously (Fassi Fehri et al., 2011; Olsson et al., 2012). PrEC cells were checked for expression of the epithelial cell markers EpCAM and E-cadherin, confirming that the primary culture did not contain any contaminating mesenchymal cells (data not shown). PrEC cells were infected with a clinical *P. acnes* prostate isolate (strain P6, type IB) at different multiplicities of infection (MOIs) and for different time points (MOI 100 for 24 and 48 h; MOI 30 for 2 weeks). Similar to previous *in vitro* infection models (Drott et al., 2010; Fassi Fehri et al., 2011; Mak et al., 2012) invasion of *P. acnes* could also be observed in PrEC cells, as judged from antibiotic protection assays and immunofluorescence microscopy of double-stained extra- and intracellular *P. acnes* (Fig. 1, Supplementary Fig. 1A). We confirmed that cell viability was not adversely affected by *P. acnes* infection at the time points tested (Supplementary Fig. 1B).

#### 3.2. Transcriptional profiles of *P. acnes*-infected PrEC cells

We decided to first monitor the global transcriptional response of PrEC cells to *P. acnes* P6 infection (MOI 100). The genome-wide transcriptional profiles at 24 h post infection (p.i.) and at 48 h p.i. were determined using microarray technology. Our analysis focused on genes that were differentially expressed between infected and non-infected cells. At 24 h p.i. a total of 1517 genes were differentially expressed with a minimum fold-change of 2.5 (674 and 843 genes were down- or upregulated after infection,

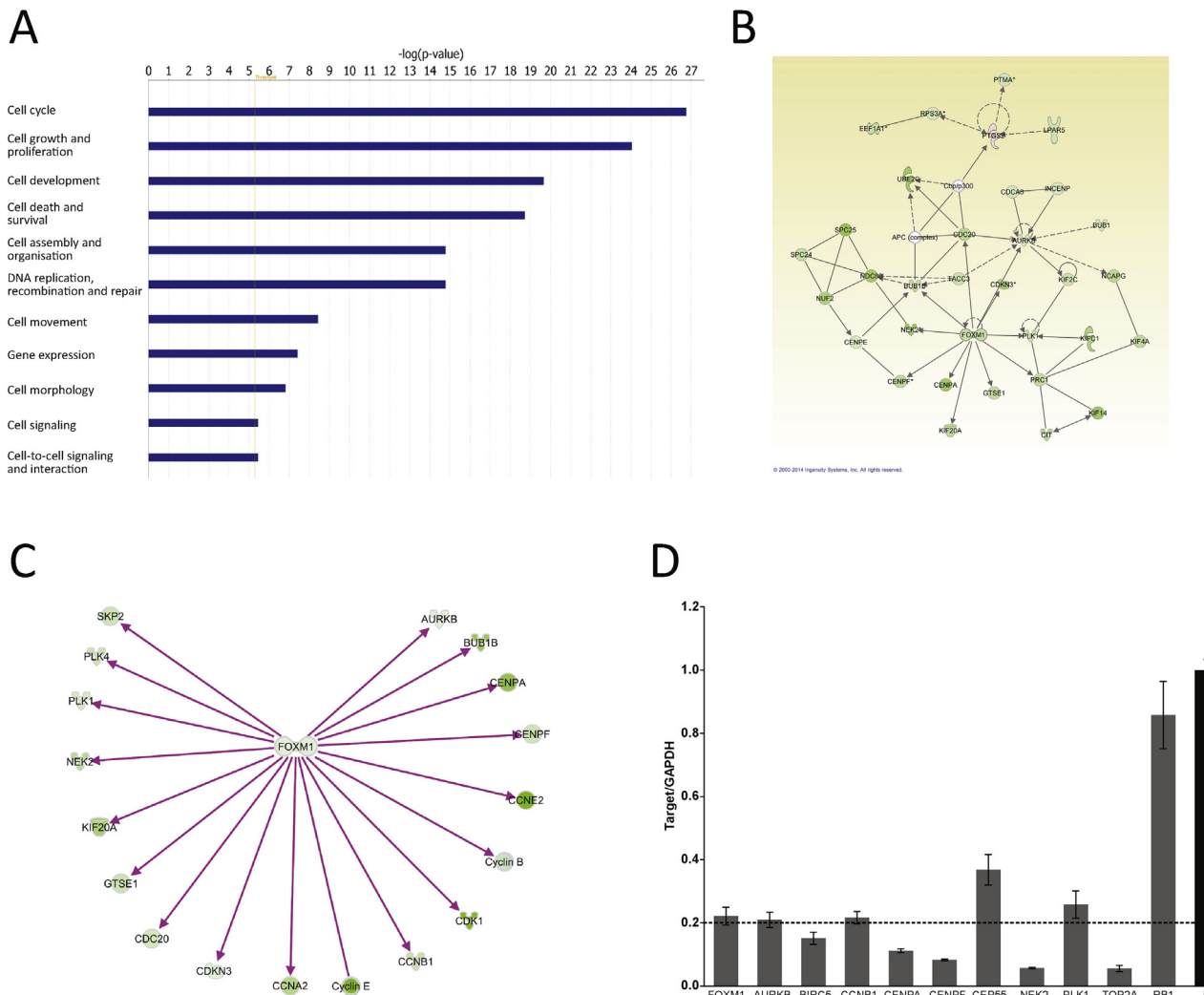


**Fig. 2.** Functional analyses of the genome-wide transcriptional response in *P. acnes*-infected PrEC cells. (A) Functional analysis of deregulated genes in PrEC cells upon *P. acnes* infection, performed with Ingenuity Pathway Analysis (IPA). *P*-values indicate significance of enrichment of cellular/molecular functions in the transcriptome at 24 h p.i. *P*-value threshold was set to 5.0E-6. Results show that the function “Cell cycle” was the most highly enriched function. All deregulated cell cycle-related genes were down-regulated. (B) IPA network analysis of deregulated genes in *P. acnes*-infected PrEC cells revealed one highly significant network (*p*-value 3.2E-13) that centers around a master regulator of cell cycle progression, FOXM1. (C) Direct targets of the FOXM1 transcription factor network involved in the G2/M transition of mitotic cell cycle were all found to be downregulated in the microarray data (green color indicates level of downregulation). (D) RT-PCR validated targets; transcript levels of the listed genes in infected cells were compared to levels in non-infected cells. Transcription of FOXM1 and most of its targets were strongly downregulated. RB1 was used as a negative control. 5-fold downregulation is indicated with a dotted line. Representative results of three independent experiments are shown.

respectively) (Supplementary Table 1A). At 48 h p.i. a total of 1100 genes were differentially expressed with a minimum fold-change of 2 (528 and 572 genes were down- or upregulated after infection, respectively) (Supplementary Table 1B). Pathway analyses of deregulated genes were carried out with the tools DAVID, STRING and Ingenuity pathway analysis (IPA). The most significant enriched cellular function among all deregulated genes at 24 h and 48 h p.i. was cell cycle (DAVID *p*-values 6.7E-8 and 1.6E-6, respectively) (Fig. 2A). 32 and 24 genes assigned to cell cycle were downregulated at 24 h and 48 h p.i., respectively (Supplementary Fig. 2A). Moreover, a String analysis showed that 50 downregulated genes are involved in kinetochore and centromere functionality, including key genes such as NDC80, NUF2, SPC25, CDC20, CENPA and CENPF (Supplementary Fig. 2B), suggesting a disturbance of the cell cycle after *P. acnes* infection. Among the upregulated genes, the most enriched KEGG pathway was cytokine–cytokine receptor interaction (*p*-values 1.0E-5 and 3.3E-2 at 24 h and 48 h p.i., respectively), as well as functionally related pathways (Toll-like receptor signaling, chemokine signaling) (data not shown). The most upreg-

ulated cytokines and chemokines were IL-1 members, IL6, IL8, CCL5, CXCL5, CXCL10, CXCL11 and CXCL14 (Supplementary Table 1). Apart from the deregulation of cell cycle-relevant genes, the data is comparable with previous work that showed that *P. acnes* can induce inflammatory processes in different host cells (Drott et al., 2010; Fassi Fehri et al., 2011; Grange et al., 2009; Mak et al., 2012). Apart from the short term infection, a 2-week infection of PrEC cells also resulted in very similar findings regarding the deregulation of cell cycle genes (Supplementary Table 1C, Supplementary Fig. 2C), indicating a persistent rather than a transient impact of *P. acnes* on the cell cycle.

### 3.3. *P. acnes* infection downregulates a master regulator of cell cycle progression, FOXM1, and its target genes

The impact of *P. acnes* on the transcription of cell cycle genes in PrEC cells prompted us to look into more detail. Pathway analyses revealed that many of the downregulated genes including Aurora B kinase (AURKB), Polo-like kinase 1 (PLK1), Cyclin B1 (CCNB1) and

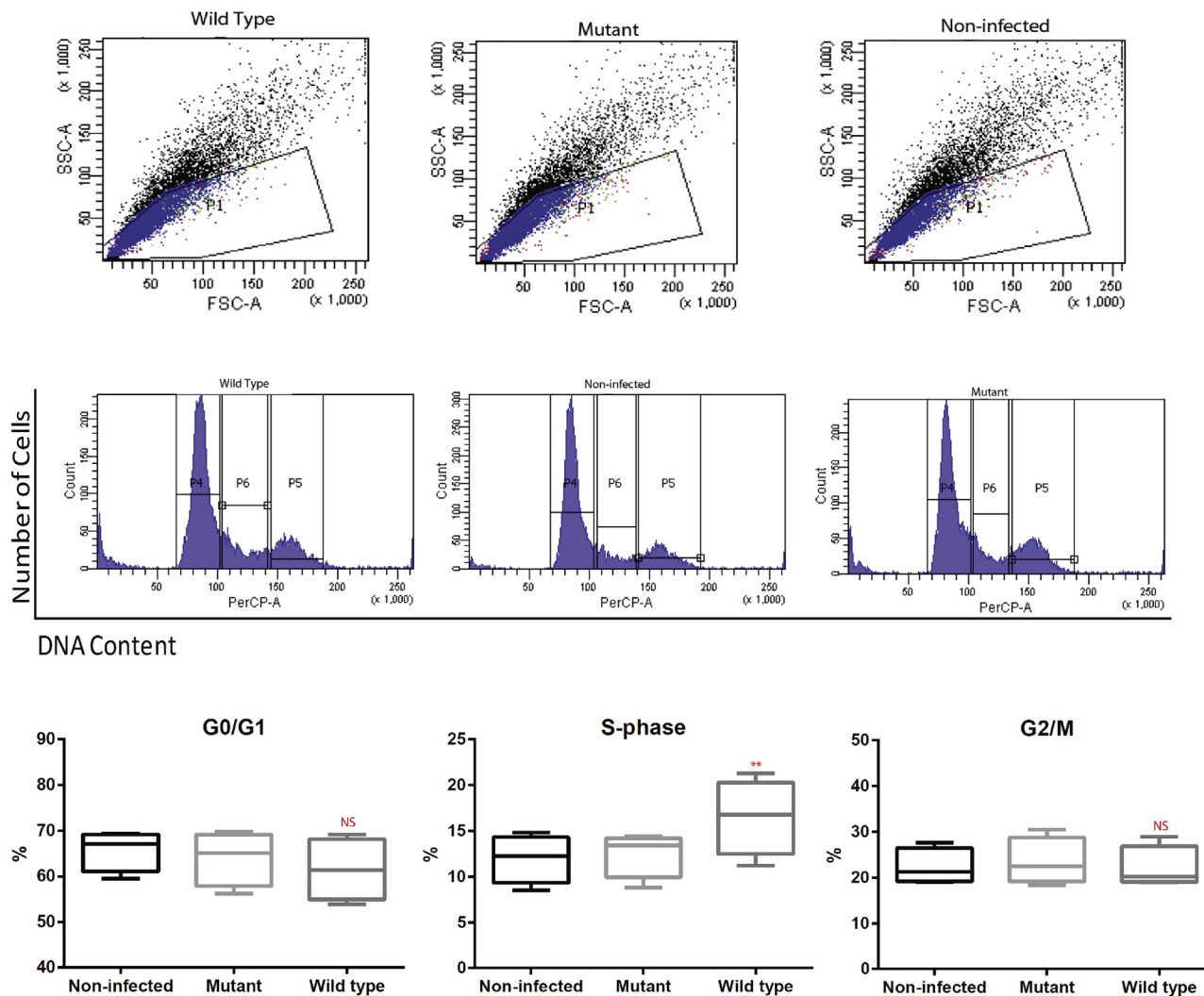


**Fig. 3.** Flow cytometry analysis of the cell cycle of PrEC cells upon *P. acnes* infection. FACS analysis with propidium iodide-stained synchronized cells was performed. *P. acnes* induced a significant increase of cells in S-phase compared to non-infected or thiopeptide deletion mutant-infected cells at 24 h p.i. No significant differences were detectable in the G0/G1 and G2/M phases. Representative results of three independent experiments are shown.

Centromere protein F (CENPF) are known to be controlled by the key regulator FOXM1, which plays a crucial role in cell proliferation and cell cycle progression (Costa, 2005; Laoukili et al., 2005; Wierstra, 2013a) (Fig. 2B and C). In agreement, FOXM1 expression was also downregulated after *P. acnes* infection (2.6-, 3- and 2.3-fold at 24 h, 48 h and 2 weeks p.i., respectively) (Supplementary Table 1). We further validated and confirmed the downregulation of FOXM1 and its direct targets in cell culture experiments using RT-PCR: FOXM1 transcription was 4–5 fold downregulated in *P. acnes*-infected PrEC cells (Fig. 2D). A known FOXM1 inhibitor, siomycin A, was used as a positive control (Gartel, 2013); at a concentration of 20 μM it downregulated FOXM1 transcription and protein expression in PrEC cells similar to *P. acnes* infection (Supplementary Fig. 3A and B).

### 3.4. *P. acnes* induces cell cycle alterations in PrEC cells

To investigate the consequences of FOXM1 downregulation, flow cytometry analyses with propidium iodide-stained cells were performed to determine the impact of *P. acnes* on cell cycle progression in PrEC cells. DNA contents of synchronized infected cells were compared to those of non-infected cells at 24 h p.i. Exposure of cells to *P. acnes* led to a statistically significant increase in the number of

cells in S-phase (Fig. 3). While 11.9% ( $\pm 2.6\%$ ) of non-infected cells were in S-phase, this increased to 16.5% ( $\pm 4.1\%$ ) upon *P. acnes* infection at 24 h p.i. ( $p < 0.05$ ; unpaired t-test). No significant differences were detectable in the G0/G1 and G2/M phases. This shows that *P. acnes* infection leads to a cell cycle disturbance in PrEC cells.

### 3.5. A thiopeptide gene cluster encoding a berninamycin A-like precursor is present in the genome of *P. acnes* P6 and other type IB strains

The thiopeptide siomycin A (produced by *Streptomyces sioyaensis*) was used as a positive control. This molecule, produced as a precursor peptide that is heavily post-translationally modified, has previously been shown to inhibit FOXM1, in addition to its function as a macrocyclic antibiotic with selective antibacterial activity against several Gram-negative and Gram-positive bacteria (Gartel, 2010, 2013; Tanaka et al., 1970). Interestingly, previous studies reported that some *P. acnes* genomes contain a gene cluster that encodes the biosynthesis of a thiopeptide with similarity to the thiopeptide biosynthesis pathway of *Streptomyces* species, in particular to siomycin A and berninamycin A biosynthesis; the latter thiopeptide is produced by *Streptomyces bernensis* (Brzuszkiewicz et al., 2011; Malcolmson et al., 2013). We searched the genome of

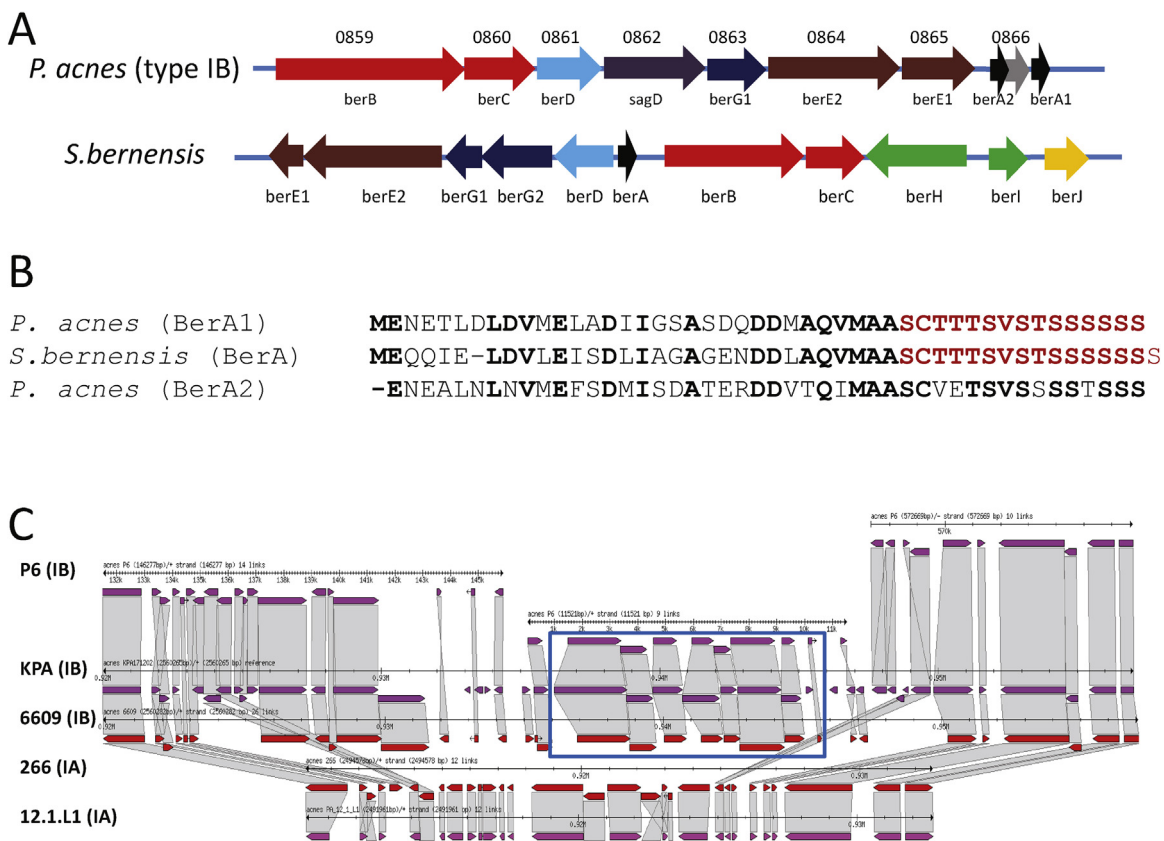


**Fig. 4.** Thiopeptide encoding genomic region. (A) Schematic representation of the thiopeptide biosynthesis-encoding gene clusters in *P. acnes* (strain KPA171202) and *S. bernensis*. In *P. acnes*, the gene cluster encodes 10 genes (PPA0859–PPA0866 and two *berA* genes), including homologs of *berABCDEG* from *S. bernensis*. The two precursor peptides are encoded by *berA1* and *berA2*; the genes are located up- and downstream of the putative gene PPA0866. (B) BerA1 of *P. acnes* possesses an almost identical copy of the 16-aa structural core peptide (in red) of berinamycin A from *S. bernensis*. BerA2 of *P. acnes* is more distantly related. (C) Comparison of the genomic region containing the thiopeptide gene cluster in five *P. acnes* strains. The thiopeptide biosynthesis gene cluster (PPA0859 to PPA0866, boxed in blue) is present in type IB strains (shown here: strains KPA171202, 6609, and P6), but absent in type IA strains (shown here: strains 12.1.L1 and 266). Please note that the genome of strain P6 is not closed. The gene alignment was done with Sybil (<http://sybil.sourceforge.net/>).

*P. acnes* strain P6 (GenBank accession number ARZZ000000000) and found an identical thiopeptide biosynthesis gene cluster to the one described in *P. acnes* KPA171202 (Fig. 4A). The gene cluster in strains P6 and KPA171202 (both type IB strains) harbors two genes (here designated *berA1* and *berA2*) that encode two different thiopeptide precursors. The one encoded by *berA1* is almost identical to the precursor peptide of berinamycin A, with the exception of a serine residue at the C-terminus (Fig. 4B).

Further analysis revealed that the thiopeptide biosynthesis gene cluster is present in the genomes of all tested type IB *P. acnes* strains, but it is absent from the genomes of strains belonging to type IA (Fig. 4C). It was reported that type IB strains have a higher antimicrobial activity against *Staphylococcus epidermidis* isolates compared with other types of *P. acnes* (Christensen et al., 2016). This could indicate that the thiopeptide produced by type IB strains has antimicrobial activity, in analogy to the main functions of siomycin A and berinamycin A of *Streptomyces* species.

### 3.6. Expression profile of thiopeptide biosynthesis genes in *P. acnes*

Characterization of the thiopeptide of *P. acnes* requires its isolation. However, all efforts to isolate the thiopeptide from *P. acnes* with HPLC-mass spectrometry approaches were unsuccessful, indicating that it is either not produced or labile. Instead, RNA-seq was used to investigate the expression of the thiopeptide biosynthesis gene cluster. This revealed that the whole cluster is expressed in the

exponential as well as stationary growth phases (Fig. 5). Strikingly, the highest transcription is associated with *berA1*. In contrast, *berA2* was not transcribed, indicating that *berA1* is the only functional thiopeptide precursor-encoding gene in *P. acnes*, at least under the growth conditions applied. Interestingly, *berA1* contains a long untranslated region (5'-UTR) that could have a regulatory function.

### 3.7. Berinamycin A is able to inhibit FOXM1 in PrEC cells, similar to *P. acnes* infection

Due to the unavailability of the *P. acnes* thiopeptide, and since BerA1 of *P. acnes* is almost 100% identical to the berinamycin A precursor peptide from *S. bernensis*, we decided to use berinamycin A for subsequent experiments. Since siomycin A and berinamycin A are similar, we hypothesized that berinamycin A is also able to inhibit FOXM1. qPCR showed that berinamycin A treatment of PrEC cells at a final concentration of 20 μM could indeed down-regulate the transcription of FOXM1 (Fig. 6A). In addition, Western blotting experiments revealed a reduction of FOXM1 protein levels in berinamycin A-treated PrEC cells compared to non-treated cells (Fig. 6B). Furthermore, the protein levels of the FOXM1 targets AURKB, PLK1 and CCNB1 were also strongly reduced in berinamycin A-treated cells, at levels comparable to the reduction observed in *P. acnes* infected cells. This suggests that a berinamycin A-like molecule produced by *P. acnes* could be responsible for the drastic effect on FOXM1 and the cell cycle in PrEC cells.

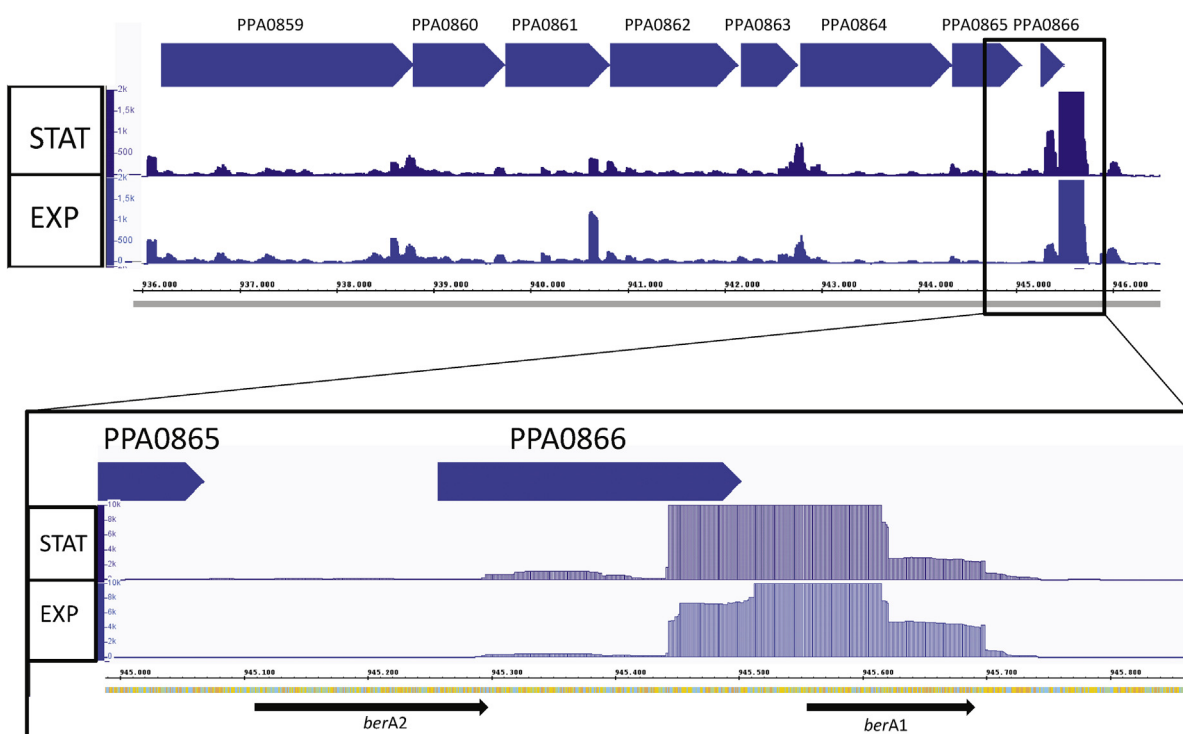


**Fig. 5.** Strong expression of *berA1*, but not *berA2* within the thilopeptide biosynthesis gene cluster of *P. acnes*. RNA-seq was applied to record the expression of the thilopeptide biosynthesis pathway-encoding gene cluster (PPA0859 to PPA0866) in *P. acnes* (strain KPA171202). Bacteria grown to exponential (EXP) and stationary (STAT) growth phases expressed the gene cluster. The most strongly expressed gene was the thilopeptide precursor-encoding gene *berA1* (see zoom-in), that possesses a long untranscribed region (5'-UTR). In contrast, *berA2* was not transcribed under the growth conditions applied.

### 3.8. Infection of PrEC cells with a thilopeptide deletion mutant does not alter FOXM1 expression and cell cycle progression

A  $\Delta$ *berA1* knockout strain was constructed in *P. acnes* KPA171202 (type IB), the only *P. acnes* strain we have so far been able to genetically modify (Sørensen et al., 2010). First, we confirmed that strains KPA171202 and P6 had the same effect on FOXM1 on gene and protein level (Supplementary Fig. 4A and B). We then tested whether mutant and wild-type strains had comparable infection properties in PrEC cells. An antibiotic protection assay showed no significant change in the ability to invade PrEC cells between wild-type and mutant strains, suggesting that the deletion had no effect on the infection capability of *P. acnes* (Supplementary Table 3). In addition, cell viability was found to be the same in PrEC cells infected with the mutant or wild-type strain (Supplementary Fig. 1B). Subsequent qPCR experiments showed that the mutant, unlike the wild-type strain, was not able to downregulate FOXM1 and selected targets (Fig. 6A). This was also observed on protein level: FOXM1, AURKB, PLK1 and CCNB1 protein levels were not reduced in cells infected with the mutant strain (Fig. 6B). In agreement, flow cytometry analysis revealed that the mutant, in contrast to the wild-type strain, was unable to change the number of cells in S-phase compared to non-infected cells (Fig. 3). Taken together, these results suggest that a berninamycin A-like thilopeptide produced by *P. acnes* is able to inhibit FOXM1 and alter cell cycle progression.

In a further experiment we used a different strain, *P. acnes* 266, belonging to the phylogroup IA. Genome analyses determined that strain 266, like other type IA strains, does not contain the thilopeptide-encoding gene cluster (Fig. 4C). Infections with strain 266 showed similar rates of bacterial invasion into PrEC cells, as observed with the other tested *P. acnes* strains (Supplementary Table 3). qPCR experiments showed that strain 266 had only a

moderate effect on FOXM1, which was downregulated <2 fold (Supplementary Fig. 4C).

## 4. Discussion

Our study investigated the response of primary human prostate cells to *P. acnes*. We focused on the ability of *P. acnes* to alter the cell cycle progression in PrEC cells. Interestingly, the analysis of downregulated genes identified many FOXM1 targets that play crucial roles in cell proliferation and cell cycle progression. Among them, we found a large network of cell cycle relevant genes that have specific structural or regulatory roles in kinetochore and centromere assembly and functionality. To our knowledge, this has not previously been described for any other bacterium-host cell interaction. Our results showed a *P. acnes*-dependent accumulation of PrEC cells in S-phase, without any apparent effect on cell viability. In this context, the location of *P. acnes* within the host cell is intriguing. Our previous studies have shown that *P. acnes* accumulates intracellularly in close proximity to the nuclear envelope in epithelial prostate cells (RWPE1) (Fassi Fehri et al., 2011; Mak et al., 2012). This location may thus turn out to be important for the bacterial impact on the cell cycle. In future experiments we will investigate if invasiveness is a prerequisite for cell cycle alterations in PrEC cells and other cell culture models.

Several other bacteria have been reported to interfere with cell cycle progression in their respective host cells. *Staphylococcus aureus* is able to induce a G2/M transition phase delay in HeLa cells (Alekseeva et al., 2013). *Shigella* was shown to cause cell cycle arrest in HeLa cells by targeting Mad2L2, an anaphase-promoting complex/cyclosome (APC) inhibitor (Iwai et al., 2007), and *Neisseria meningitidis* causes cell cycle arrest of human brain endothelial cells at S-phase (Oosthuysen et al., 2015). Host cell cycle perturbation was also observed upon infections with *Listeria monocytogenes* and *Helicobacter pylori* (Fehri et al., 2009; Leitao et al., 2014). In

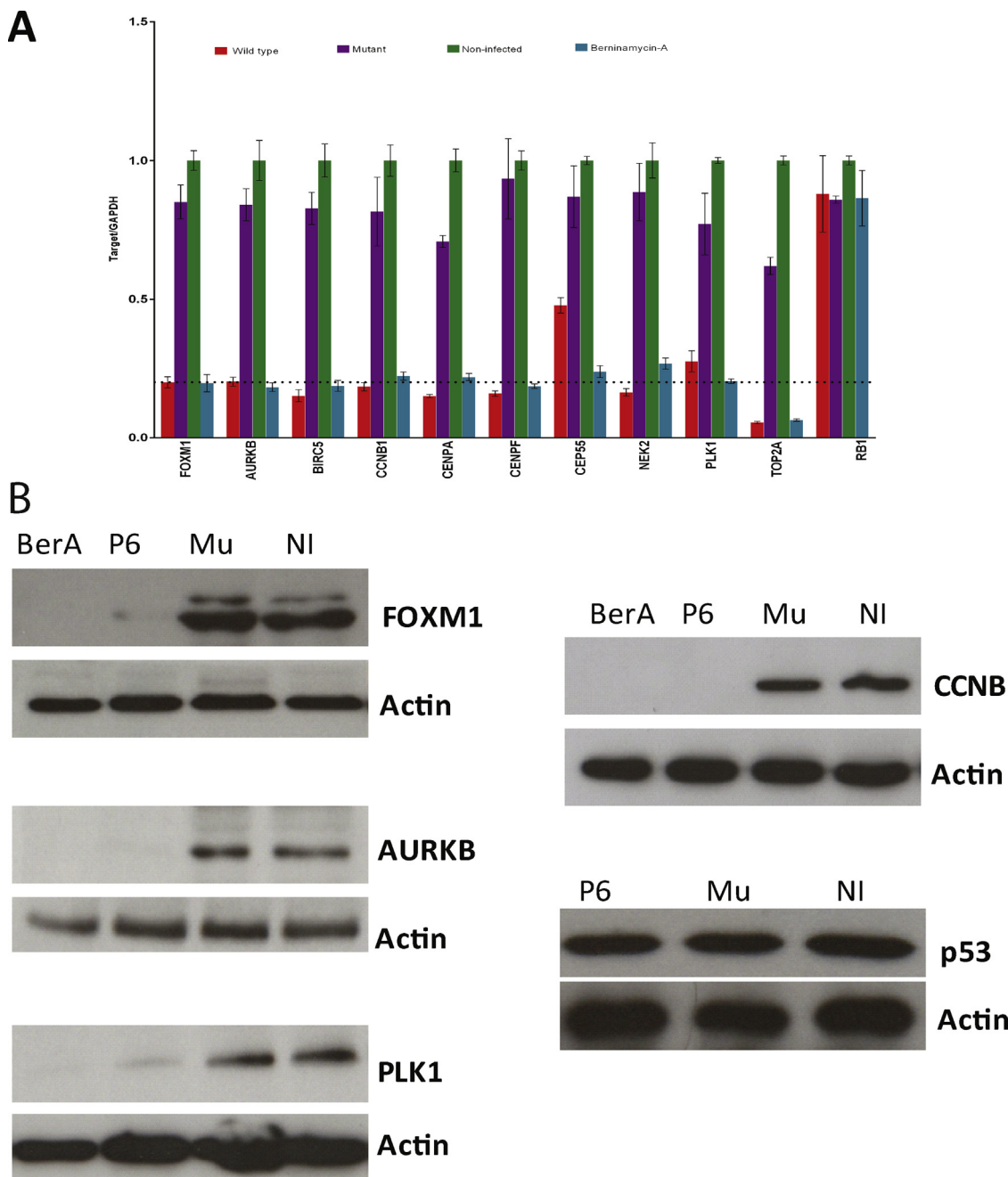


**Fig. 6.** A thilopeptide deletion mutant of *P. acnes* does not alter transcript and protein levels of FOXM1 and its targets in PrEC cells. (A) RT-PCR for FOXM1 mRNA and its direct targets was carried out in PrEC cells treated with berinamycin A ( $20 \mu\text{M}$ ) or infected for 24 h with *P. acnes* wild-type (strain KPA171202) and the thilopeptide-deletion mutant strain (Mu). Transcript levels of the listed genes are downregulated in berinamycin A-treated and in wild-type strain-infected, but not in mutant strain-infected PrEC cells. Infection had no effect on expression of RB1. A 5-fold downregulation is marked with a dotted line. Three independent experiments were performed. (B) *P. acnes* wild-type strain infection, as well as treatment of cells with  $20 \mu\text{M}$  berinamycin A for 24 h inhibits the production of FOXM1, AURKB, PLK1 and CCNB in infected PrEC cells, compared to non-infected (NI) cells. In contrast to the wild-type strain, infections with the thilopeptide deletion mutant did not reduce protein levels of FOXM1 and its tested targets in PrEC cells. Protein levels of p53 were not altered in wild-type or mutant-infected compared to non-infected PrEC cells. Representative results of three independent experiments are shown.

most studies the exact mechanisms by which bacteria interfere with the cell cycle are not known. Regarding the biological significance, it has been suggested that pathogen-induced host cell cycle alteration serves the pathogen to better colonize and propagate, for instance by delaying epithelial renewal or reducing host cell defense functions (Alekseeva et al., 2013; Iwai et al., 2007).

Our study indicates that *P. acnes* has a distinct mechanism to alter the cell cycle, i.e., by inhibiting FOXM1 in a thilopeptide-dependent manner. Thilopeptides, also called thiazoly peptides,

have multiple functions; in addition to their innate antibacterial activity, they can for example have anti-cancer, anti-plasmodial and immunosuppressive activities. Thiomycin and siomycin A produced by *Streptomyces* species are known FOXM1 inhibitors (Bhat et al., 2009; Gartel, 2013; Radhakrishnan et al., 2006) that are able to down-regulate the transcriptional activity as well as the protein and mRNA abundance of FOXM1 via proteasome inhibition. Their major *in vivo* role is most likely as macrocyclic antibiotics with potent and selective antibacterial activity against Gram-negative

and Gram-positive bacteria (Tanaka et al., 1970). Berninamycin A produced by *S. bernensis* is similar to siomycin A and has been shown to act as an antibiotic too, thereby acting as a vigorous inhibitor of protein synthesis in Gram-positive bacteria (Reusser, 1969; Thompson et al., 1982).

We show here that in analogy to siomycin A, berninamycin A can also act as a FOXM1 inhibitor. FOXM1 has diverse key roles in eukaryotic cells including the regulation of many G2/M-specific genes that are essential for chromosome stability. FOXM1 downregulation leads to pleiotropic cell cycle defects, including a delay in G2, chromosome mis-segregation and frequent failure of cytokinesis (Wierstra, 2013a,b). For instance, FOXM1 activates transcription of cyclin B, which is essential for a timely mitotic entry, whereas CENP-F, another direct target of FOXM1, is essential for precise functioning of the mitotic spindle checkpoint (Costa, 2005). Thus, by downregulating FOXM1 in PrEC cells, *P. acnes* is able to exert a profound effect on cell cycle progression, most likely due to perturbations of kinetochore and centromere assembly and functionality.

The *in vivo* significance of this study remains to be determined. Assuming that the bacterium is encountering and invading primary epithelial cells of human prostates, as suggested by previous studies (Alexeyev et al., 2007; Bae et al., 2014; Cohen et al., 2005; Fassi Fehri et al., 2011; Mak et al., 2012, 2013; Shinohara et al., 2013), we have to take two different responses and thus scenarios into consideration.

One response is triggered by the bacterium's pro-inflammatory activity on prostate epithelial cells (Drott et al., 2010; Fassi Fehri et al., 2011; Mak et al., 2012), resulting in the release of chemokines and cytokines, including IL-6. Previous work suggested that this inflammatory response induces cell proliferation and anchorage-independent growth of infected cells, thus supporting cellular transformation (Fassi Fehri et al., 2011). The outcome depends on the severity and duration of the inflammation; some evidence exists that *P. acnes* is able to establish a persistent infection rather than a transient one (Mak et al., 2012; Shinohara et al., 2013). Important for the outcome will also be the individual contributions of innate and adaptive immunity. Apart from the long-term secretion of inflammatory mediators during a persistent infection, adaptive immunity is activated, potentially involving *P. acnes*-specific Th1 and Th17 responses, as seen in inflamed skin (Kistowska et al., 2015).

The second response, i.e. the impact of *P. acnes* on FOXM1 and the cell cycle as outlined in this report, points towards an opposing consequence of a *P. acnes* infection. By blocking cell cycle progression, cells might be silenced and eventually eliminated, thus reducing the risk of cellular survival and proliferation and eventual transformation. In line with this, inhibition of FOXM1 and its targets have been suggested as anti-tumor therapy (Briest et al., 2015; Jiang et al., 2015; Miao et al., 2014). In this regard, it should be mentioned that *P. acnes* was used in anti-cancer therapies in the 70 s and 80 s of the last century (Halpern et al., 1966; Smith and Woodruff, 1968). The anti-tumor activity has mainly been attributed to a *P. acnes*-triggered Th1 response (Tsuda et al., 2011), but a more direct bacterial effect on the cellular fate may be involved as well. Interestingly, another study supported the assumption of a possible anti-cancer effect of *P. acnes*: it was observed that higher anti-*P. acnes* antibody titers were inversely associated with prostate cancer risk (Severi et al., 2010). Our study suggests that this second, anti-cancer scenario of *P. acnes* is phylotype-dependent: only thiopeptide-producing type IB strains would exert this effect on the cell cycle, but not strains of type IA, the most abundant phylotype on human skin. In this regard, type IA and IB strains have been differently associated with disease or health, respectively, and these types induce different host cell responses (Fitz-Gibbon et al., 2013; Lomholt and Kilian, 2010; Nagy et al., 2005; Rollason et al., 2013). It remains to be seen if the thiopeptide-producing ability of *P. acnes*

type IB results in a host beneficial effect or at least in reduced pathogenesis. A recent study has investigated the phylotype distribution of *P. acnes* strains isolated from cancerous prostates (100 cases): Most strains belonged to type II (51%), followed by type IA (27%) (Davidsson et al., 2016). Both types do not possess the thiopeptide gene cluster. In contrast, only 15% of the isolate strains belonged to type IB. This suggests that the majority of *P. acnes* strains present in cancerous prostates do not possess the capability of thiopeptide-mediated FOXM1 inhibition.

Elucidating the long-term fate of host cells following infection with *P. acnes* will be a future focus of interest. Initial data suggest that arrested cells do not undergo apoptosis. Instead, host cell fate might be driven towards senescence. This is in accordance with observations showing that FOXM1 prevents cellular senescence and FOXM1 degradation leads to cellular senescence. Likewise, downregulation of the FOXM1 targets PLK1 or SKP2 induces senescence in primary cells (Kim et al., 2013; Lin et al., 2010). Since inhibition of FOXM1 is currently discussed in anti-cancer therapy (Bella et al., 2014; Halasi and Gartel, 2013), the identification of new inhibitors is of crucial interest. Our study introduces a promising new FOXM1 inhibitor, provided that the *P. acnes* thiopeptide can be purified to study its bioactivity in depth.

## Author contributions

**Conception and design:** B. S. and H. B.

**Development of methodology:** B. S. and H. B.

**Acquisition of data:** B. S., M. A. A. and G. J. M. C.

**Analysis and interpretation of data:** B. S. and H. B.

**Writing, review, and/or revision of the manuscript:** B. S., H. B., and T. F. M.

**Study supervision:** T. F. M.

**Provided microarray analyses:** H.-J. M.

## Acknowledgments

The authors thank Flow Cytometry Core Facility staff, especially Toralf Kaiser for his support with FACS data analysis, Robert Hurwitz for support with mass spectrometry data analysis, Erik González for acquiring automated microscopy images, Hilmar Berger for scientific discussions, Ina Wagner and Meike Sørensen for excellent technical assistance and Rike Zietlow for editing the manuscript. This work was partially funded by the Danish Council for Independent Research (to HB).

The authors have no conflict of interest to declare.

## Appendix A. Supplementary data

Supplementary data associated with this article can be found, in the online version, at <http://dx.doi.org/10.1016/j.ijmm.2016.06.006>.

## References

- Agak, G.W., Qin, M., Nobe, J., Kim, M.H., Krutzik, S.R., Tristan, G.R., Elashoff, D., Garban, H.J., Kim, J., 2014. *Propionibacterium acnes* induces an IL-17 response in acne vulgaris that is regulated by vitamin A and vitamin D. *J. Invest. Dermatol.* 134, 366–373.
- Alekseeva, L., Rault, L., Almeida, S., Legembre, P., Edmond, V., Azevedo, V., Miyoshi, A., Even, S., Taieb, F., Arlot-Bonnemains, Y., Le Loir, Y., Berkova, N., 2013. *Staphylococcus aureus*-induced G2/M phase transition delay in host epithelial cells increases bacterial infective efficiency. *PLoS One* 8, e63279.
- Alexeyev, O.A., Marklund, I., Shannon, B., Golovleva, I., Olsson, J., Andersson, C., Eriksson, I., Cohen, R., Elgh, F., 2007. Direct visualization of *Propionibacterium acnes* in prostate tissue by multicolor fluorescent *in situ* hybridization assay. *J. Clin. Microbiol.* 45, 3721–3728.
- Bae, Y., Ito, T., Iida, T., Uchida, K., Sekine, M., Nakajima, Y., Kumagai, J., Yokoyama, T., Kawachi, H., Akashi, T., Eishi, Y., 2014. Intracellular *Propionibacterium acnes*

- infection in glandular epithelium and stromal macrophages of the prostate with or without cancer. *PLoS One* 9, e90324.
- Belkaid, Y., Segre, J.A., 2014. Dialogue between skin microbiota and immunity. *Science* 346, 954–959.
- Bella, L., Zona, S., Nestal de Moraes, G., Lam, E.W., 2014. FOXM1: a key oncofoetal transcription factor in health and disease. *Semin. Cancer Biol.* 29, 32–39.
- Bhat, U.G., Halasi, M., Gartel, A.L., 2009. FoxM1 is a general target for proteasome inhibitors. *PLoS One* 4, e6593.
- Brüggemann, H., Henne, A., Hostler, F., Liesegang, H., Wiezer, A., Strittmatter, A., Hüjer, S., Durre, P., Gottschalk, G., 2004. The complete genome sequence of *Propionibacterium acnes*, a commensal of human skin. *Science* 305, 671–673.
- Briest, F., Berg, E., Grass, I., Freitag, H., Kaemmerer, D., Lewens, F., Christen, F., Arsenic, R., Altendorf-Hofmann, A., Kunze, A., Sanger, J., Knosel, T., Siegmund, B., Hummel, M., Grabowski, P., 2015. FOXM1: a novel drug target in gastroenteropancreatic neuroendocrine tumors. *Oncotarget* 6, 8185–8199.
- Brzuszkiewicz, E., Weiner, J., Wollherr, A., Thurmer, A., Hupedes, J., Lomholt, H.B., Kilian, M., Gottschalk, G., Daniel, R., Mollenkopf, H.J., Meyer, T.F., Brüggemann, H., 2011. Comparative genomics and transcriptomics of *Propionibacterium acnes*. *PLoS One* 6, e21581.
- Christensen, G.J., Scholz, C.F., Enghild, J., Rohde, H., Kilian, M., Thurmer, A., Brzuszkiewicz, E., Lomholt, H.B., Brüggemann, H., 2016. Antagonism between *Staphylococcus epidermidis* and *Propionibacterium acnes* and its genomic basis. *BMC Genom.* 17, 152.
- Churchill, G.A., 2002. Fundamentals of experimental design for cDNA microarrays. *Nat. Genet.* 32 (Suppl), 490–495.
- Cohen, R.J., Shannon, B.A., McNeal, J.E., Shannon, T., Garrett, K.L., 2005. *Propionibacterium acnes* associated with inflammation in radical prostatectomy specimens: a possible link to cancer evolution? *J. Urol.* 173, 1969–1974.
- Costa, R.H., 2005. FoxM1 dances with mitosis. *Nat. Cell Biol.* 7, 108–110.
- Davidsson, S., Molling, P., Rider, J.R., Unemo, M., Karlsson, M.G., Carlsson, J., Andersson, S.O., Elgh, F., Soderquis, B., Andren, O., 2016. Frequency and typing of *Propionibacterium acnes* in prostate tissue obtained from men with and without prostate cancer. *Infect. Agent Cancer* 11, 26.
- Drott, J.B., Alexeyev, O., Bergstrom, P., Elgh, F., Olsson, J., 2010. *Propionibacterium acnes* infection induces upregulation of inflammatory genes and cytokine secretion in prostate epithelial cells. *BMC Microbiol.* 10, 126.
- Dugar, G., Herbig, A., Forstner, K.U., Heidrich, N., Reinhardt, R., Nieselt, K., Sharma, C.M., 2013. High-resolution transcriptome maps reveal strain-specific regulatory features of multiple *Campylobacter jejuni* isolates. *PLoS Genet.* 9, e1003495.
- Eishi, Y., 2013. Etiologic link between sarcoidosis and *Propionibacterium acnes*. *Respir. Investig.* 51, 56–68.
- Fassi Fehri, L., Mak, T.N., Laube, B., Brinkmann, V., Ogilvie, L.A., Mollenkopf, H., Lein, M., Schmidt, T., Meyer, T.F., Brüggemann, H., 2011. Prevalence of *Propionibacterium acnes* in diseased prostates and its inflammatory and transforming activity on prostate epithelial cells. *Int. J. Med. Microbiol.* 301, 69–78.
- Fehri, L.F., Rechner, C., Janssen, S., Mak, T.N., Holland, C., Bartfeld, S., Brüggemann, H., Meyer, T.F., 2009. Helicobacter pylori-induced modification of the histone H3 phosphorylation status in gastric epithelial cells reflects its impact on cell cycle regulation. *Epigenetics* 4, 577–586.
- Fitz-Gibbon, S., Tomida, S., Chiu, B.H., Nguyen, L., Du, C., Liu, M., Elashoff, D., Erfe, M.C., Loncaric, A., Kim, J., Modlin, R.L., Miller, J.F., Sodergren, E., Craft, N., Weinstock, G.M., Li, H., 2013. *Propionibacterium acnes* strain populations in the human skin microbiome associated with acne. *J. Invest. Dermatol.* 133, 2152–2160.
- Gartel, A.L., 2010. A new target for proteasome inhibitors: FoxM1. *Expert Opin. Investig. Drugs* 19, 235–242.
- Gartel, A.L., 2013. Thiazole antibiotics siomycin a and thiostrepton inhibit the transcriptional activity of FOXM1. *Front. Oncol.* 3, 150.
- Grange, P.A., Chereau, C., Raingeaud, J., Nicco, C., Weill, B., Dupin, N., Batteux, F., 2009. Production of superoxide anions by keratinocytes initiates *P. acnes*-induced inflammation of the skin. *PLoS Pathog.* 5, e1000527.
- Halasi, M., Gartel, A.L., 2013. FOX(M1) news—it is cancer. *Mol. Cancer Ther.* 12, 245–254.
- Halpern, B.N., Biozzi, G., Stiffel, C., Mouton, D., 1966. Inhibition of tumour growth by administration of killed *Corynebacterium parvum*. *Nature* 212, 853–854.
- Iwai, H., Kim, M., Yoshikawa, Y., Ashida, H., Ogawa, M., Fujita, Y., Muller, D., Kirikae, T., Jackson, P.K., Kotani, S., Sasakawa, C., 2007. A bacterial effector targets Mad2L2, an APC inhibitor, to modulate host cell cycling. *Cell* 130, 611–623.
- Jiang, L., Wu, X., Wang, P., Wen, T., Yu, C., Wei, L., Chen, H., 2015. Targeting FoxM1 by thiostrepton inhibits growth and induces apoptosis of laryngeal squamous cell carcinoma. *J. Cancer Res. Clin. Oncol.* 141, 971–981.
- Kim, H.J., Cho, J.H., Kim, J.R., 2013. Downregulation of Polo-like kinase 1 induces cellular senescence in human primary cells through a p53-dependent pathway. *J. Gerontol. A Biol. Sci. Med. Sci.* 68, 1145–1156.
- Kistowska, M., Gehrke, S., Jankovic, D., Kerl, K., Fettelschoss, A., Feldmeyer, L., Fenini, G., Kolios, A., Navarini, A., Ganceviciene, R., Schaubert, J., Contassot, E., French, L.E., 2014. IL-1 $\beta$  drives inflammatory responses to *Propionibacterium acnes* in vitro and in vivo. *J. Invest. Dermatol.* 134, 677–685.
- Kistowska, M., Meier, B., Proust, T., Feldmeyer, L., Cozzio, A., Kuendig, T., Contassot, E., French, L.E., 2015. *Propionibacterium acnes* promotes Th17 and Th17/Th1 responses in acne patients. *J. Invest. Dermatol.* 135, 110–118.
- Laoukili, J., Kooistra, M.R., Brás, A., Kauw, J., Kerkhoven, R.M., Morrison, A., Clevers, H., Medema, R.H., 2005. FoxM1 is required for execution of the mitotic programme and chromosome stability. *Nat. Cell Biol.* 7, 126–136.
- Leitao, E., Costa, A.C., Brito, C., Costa, L., Pombinho, R., Cabanes, D., Sousa, S., 2014. *Listeria monocytogenes* induces host DNA damage and delays the host cell cycle to promote infection. *Cell Cycle* 13, 928–940.
- Lin, H.K., Chen, Z., Wang, G., Nardella, C., Lee, S.W., Chan, C.H., Yang, W.L., Wang, J., Egia, A., Nakayama, K.I., Cordon-Cardo, C., Teruya-Feldstein, J., Pandolfi, P.P., 2010. Skp2 targeting suppresses tumorigenesis by Arf-p53-independent cellular senescence. *Nature* 464, 374–379.
- Lomholt, H.B., Kilian, M., 2010. Population genetic analysis of *Propionibacterium acnes* identifies a subpopulation and epidemic clones associated with acne. *PLoS One* 5, e12277.
- Mak, T.N., Fischer, N., Laube, B., Brinkmann, V., Metruccio, M.M., Sfanos, K.S., Mollenkopf, H.J., Meyer, T.F., Brüggemann, H., 2012. *Propionibacterium acnes* host cell tropism contributes to vimentin-mediated invasion and induction of inflammation. *Cell. Microbiol.* 14, 1720–1733.
- Mak, T.N., Sfanos, K.S., Brüggemann, H., 2013. Draft genome sequences of two strains of *Propionibacterium acnes* isolated from radical prostatectomy specimens. *Genome Announc.* 1.
- Malcolmson, S.J., Young, T.S., Ruby, J.G., Skewes-Cox, P., Walsh, C.T., 2013. The posttranslational modification cascade to the thiopeptide bermamycin generates linear forms and altered macrocyclic scaffolds. *Proc. Natl. Acad. Sci. U. S. A.* 110, 8483–8488.
- McDowell, A., Barnard, E., Nagy, I., Gao, A., Tomida, S., Li, H., Eady, A., Cove, J., Nord, C.E., Patrick, S., 2012. An expanded multilocus sequence typing scheme for *Propionibacterium acnes*: investigation of ‘pathogenic’, ‘commensal’ and antibiotic-resistant strains. *PLoS One* 7, e41480.
- McDowell, A., Nagy, I., Magyari, M., Barnard, E., Patrick, S., 2013. The opportunistic pathogen *Propionibacterium acnes*: insights into typing, human disease, clonal diversification and CAMP factor evolution. *PLoS One* 8, e70897.
- Miao, L., Xiong, X., Lin, Y., Cheng, Y., Lu, J., Zhang, J., Cheng, N., 2014. Down-regulation of FoxM1 leads to the inhibition of the epithelial-mesenchymal transition in gastric cancer cells. *Cancer Genet.* 207, 75–82.
- Nagy, I., Pivarcsi, A., Koreck, A., Szell, M., Urban, E., Kemeny, L., 2005. Distinct strains of *Propionibacterium acnes* induce selective human beta-defensin-2 and interleukin-8 expression in human keratinocytes through toll-like receptors. *J. Invest. Dermatol.* 124, 931–938.
- Nicol, J.W., Helt, G.A., Blanchard Jr., S.G., Raja, A., Loraine, A.E., 2009. The integrated genome browser: free software for distribution and exploration of genome-scale datasets. *Bioinformatics* 25, 2730–2731.
- Olsson, J., Drott, J.B., Laurantzon, L., Laurantzon, O., Bergh, A., Elgh, F., 2012. Chronic prostatic infection and inflammation by *Propionibacterium acnes* in a rat prostate infection model. *PLoS One* 7, e51434.
- Oosthuysen, W.F., Mueller, T., Dittrich, M.T., Schubert-Urkmeir, A., 2015. *Neisseria meningitidis* causes cell cycle arrest of human brain microvascular endothelial cells at S phase via p21 and cyclin G2. *Cell. Microbiol.* 18, 46–65.
- Perry, A., Lambert, P., 2011. *Propionibacterium acnes*: infection beyond the skin. *Expert Rev. Antic. Infect. Ther.* 9, 1149–1156.
- Pozarowski, P., Darzynkiewicz, Z., 2004. Analysis of cell cycle by flow cytometry. *Methods Mol. Biol.* 281, 301–311.
- Qin, M., Pirouz, A., Kim, M.H., Krutzik, S.R., Garban, H.J., Kim, J., 2014. *Propionibacterium acnes* induces IL-1 $\beta$  secretion via the NLRP3 inflammasome in human monocytes. *J. Invest. Dermatol.* 134, 381–388.
- Radhakrishnan, S.K., Bhat, U.G., Hughes, D.E., Wang, I.C., Costa, R.H., Gartel, A.L., 2006. Identification of a chemical inhibitor of the oncogenic transcription factor forkhead box M1. *Cancer Res.* 66, 9731–9735.
- Reusser, F., 1969. Mode of action of bermamycin: an inhibitor of protein biosynthesis. *Biochemistry* 8, 3303–3308.
- Rollason, J., McDowell, A., Albert, H.B., Barnard, E., Worthington, T., Hilton, A.C., Vernallis, A., Patrick, S., Elliott, T., Lambert, P., 2013. Genotypic and antimicrobial characterisation of *Propionibacterium acnes* isolates from surgically excised lumbar disc herniations. *Biomed. Res. Int.* 2013, 530382.
- Sobel, R.E., Wang, Y., Sadar, M.D., 2006. Molecular analysis and characterization of PrEC, commercially available prostate epithelial cells. *In Vitro Cell. Dev. Biol. Anim.* 42, 33–39.
- Sörensen, M., Mak, T.N., Hurwitz, R., Ogilvie, L.A., Mollenkopf, H.J., Meyer, T.F., Brüggemann, H., 2010. Mutagenesis of *Propionibacterium acnes* and analysis of two CAMP factor knock-out mutants. *J. Microbiol. Methods* 83, 211–216.
- Severi, G., Shannan, B.A., Hoang, H.N., Baglietto, L., English, D.R., Hopper, J.L., Pedersen, J., Southey, M.C., Sinclair, R., Cohen, R.J., Giles, G.G., 2010. Plasma concentration of *Propionibacterium acnes* antibodies and prostate cancer risk: results from an Australian population-based case-control study. *Br. J. Cancer* 103, 411–415.
- Sharma, C.M., Hoffmann, S., Darfeuille, F., Reignier, J., Findeiss, S., Sittka, A., Chabas, S., Reiche, K., Hackermuller, J., Reinhardt, R., Stadler, P.F., Vogel, J., 2010. The primary transcriptome of the major human pathogen *Helicobacter pylori*. *Nature* 464, 250–255.
- Shinohara, D.B., Vaghshnia, A.M., Yu, S.H., Mak, T.N., Brüggemann, H., Nelson, W.G., De Marzo, A.M., Yegnasubramanian, S., Sfanos, K.S., 2013. A mouse model of chronic prostatic inflammation using a human prostate cancer-derived isolate of *Propionibacterium acnes*. *Prostate* 73, 1007–1015.
- Smith, L.H., Woodruff, M.F., 1968. Comparative effect of two strains of *C. parvum* on phagocytic activity and tumour growth. *Nature* 219, 197–198.
- Tanaka, K., Watanabe, S., Teraoka, H., Tamaki, M., 1970. Effect of siomycin on protein synthesizing activity of *Escherichia coli* ribosomes. *Biochem. Biophys. Res. Commun.* 39, 1189–1193.

- Thompson, J., Cundliffe, E., Stark, M.J., 1982. The mode of action of berninamycin and mechanism of resistance in the producing organism, *Streptomyces bernensis*. *J. Gen. Microbiol.* **128**, 875–884.
- Tsuda, K., Yamanaka, K., Linan, W., Miyahara, Y., Akeda, T., Nakanishi, T., Kitagawa, H., Kakeda, M., Kurokawa, I., Shiku, H., Gabazza, E.C., Mizutani, H., 2011. Intratumoral injection of *Propionibacterium acnes* suppresses malignant melanoma by enhancing Th1 immune responses. *PLoS One* **6**, e29020.
- Wierstra, I., 2013a. FOXM1 (Forkhead box M1) in tumorigenesis: overexpression in human cancer, implication in tumorigenesis, oncogenic functions, tumor-suppressive properties, and target of anticancer therapy. *Adv. Cancer Res.* **119**, 191–419.
- Wierstra, I., 2013b. The transcription factor FOXM1 (Forkhead box M1): proliferation-specific expression, transcription factor function, target genes, mouse models, and normal biological roles. *Adv. Cancer Res.* **118**, 97–398.